Conference materials
UDC 535.42
DOI: https://doi.org/10.18721/JPM.163.205

A new method for calculating spectral diffractive lenses for focusing laser radiation of various wave lengths

S.A. Goranskaia[1]✉

[1] Saint Petersburg State University of Telecommunications named after prof. M.A. Bonch-Bruevich, St. Petersburg, Russia

✉ svetlancho.zueva@yandex.ru

Abstract. The necessity of developing a new methodology for calculating diffractive spectral lenses for optical systems with variable wavelength laser radiation is substantiated. The method for calculating spectral diffraction lenses for focusing radiation of different wavelengths at specified focal points has been developed. The method for calculating cascade metal-dielectric layered structures for optical filtering has been developed, and a method for obtaining neural network descriptors applicable to the analysis of hyperspectral data has been developed. Calculation examples for various designs of optical diffractive lenses are presented. The optimal parameters for the designs of diffractive lenses are established.

Keywords: Spectral diffraction lenses, focus, focal plane, efficiency assessment, microrelief of spectral diffraction lenses

Citation: Goranskaia S.A., A new method for calculating spectral diffractive lenses for focusing laser radiation of various wave lengths, St. Petersburg State Polytechnical University Journal. Physics and Mathematics. 16 (3.2) (2023) 33–38. DOI: https://doi.org/10.18721/JPM.163.205

Материалы конференции
УДК 535.42
DOI: https://doi.org/10.18721/JPM.163.205

Новая методика расчета спектральных дифракционных линз для фокусировки лазерного излучения различных длин волн

С.А. Горанская[1]✉

[1] Санкт-Петербургский государственный университет телекоммуникаций им. проф. М. А. Бонч-Бруевича, Санкт-Петербург, Россия

✉ svetlancho.zueva@yandex.ru

Аннотация. Разработан метод расчета спектральных дифракционных линз для фокусировки излучения разных длин волн в заданных точках фокуса. Разработан метод расчета каскадных металлодиэлектрических слоистых структур для оптической фильтрации, а также метод получения нейросетевых дескрипторов, применимых для анализа гиперспектральных данных. Представлены примеры расчета для различных конструкций оптических дифракционных линз. Установлены оптимальные параметры для конструкций дифракционных линз.

Ключевые слова: спектральные дифракционные линзы, фокус, фокальная плоскость, длина волны, оценка эффективности, микрорельеф спектральных дифракционных линз

Ссылка при цитировании: Горанская С.А. Новая методика расчета спектральных дифракционных линз для фокусировки лазерного излучения различных длин волн // Научно-технические ведомости СПбГПУ. Физико-математические науки. 2023. Т. 16. № 3.2. С. 33–38. DOI: https://doi.org/10.18721/JPM.163.205

Introduction

Various models of refractive lenses are actively being used in modern optical devices [1–7]. The increasing demand for precise measurements of various parameters using optical devices, such as night vision devices or refractometers, has led to several challenges [6–12]. Refractive lenses that focus incident radiation often suffer from a significant drawback – dispersion of focal length for different wavelengths of the incident radiation. Consequently, their usage is limited to only one radiation wavelength, especially when dealing with lasers [12–14].

Another drawback that restricts their use in compact optical systems is their thickness. To overcome this limitation, diffractive lenses (DL) are employed. These lenses have a diffraction relief thickness comparable to the incident wavelength of the radiation. They find application in the development of compact imaging systems for mobile devices and unmanned aerial vehicles, particularly when multiple wavelengths are emitted simultaneously – spectral diffractive lenses (SDLs).

One well-known type of diffraction lens operating at multiple wavelengths is the harmonic diffraction lens (HDL), which possesses m times higher diffraction microrelief and allows focusing several different wavelengths into the same focus using different orders of diffraction [13, 15–17]. However, the operating wavelengths of the SDL cannot be arbitrarily chosen; they must satisfy an analytical relation depending on *m* and the 'main' operating wavelength.

Calculation Method of the SDL for Focusing Radiation of Different Wavelengths. The calculation of the SDL is performed independently for each point using the formula:

$$h_j = h_{\max}\frac{q_j}{Q},\ q_j = \underset{q\in\{0,\dots,Q-1\}}{\arg\min}\left[\sum_{l=1}^{L} w_l \left| T_{sl}\left(h_{\max}\frac{q}{Q};\lambda_l\right) - T_l\left(u_j;\lambda_l,x_l\right)\right|^2\right]. \quad (1)$$

The calculation of microrelief height at each point by full brute force is simple from the computational point of view, as it corresponds to the calculation of Q weighted sums L of differences of two exponents. In a particular case, the coordinates of the focal points may coincide: $x_l = (x_0, y_0)$, $l = 1,\dots, L$. In this case, this method of calculating the SDL results in an 'achromatic' SDL, focusing radiation of different wavelengths to the same fixed point. This approach is most rational for short-focus lenses, which are used in fiber systems, optical fibers, optical correlators, and near-IR photodetectors. Works [18–21] utilize a zone approach to image formation at different wavelengths, which is more optimal for lenses with long and medium focus, used to solve different problems than those considered in my work.

Modified Infrared Slope Index

To evaluate the effectiveness of this method, we calculated the SDL focusing two wavelengths $\lambda_1 = 455$ nm and $\lambda_1 = 750$ nm into two points in the plane $z = f = 750$ mm at the coordinates $x_1 = (-x_1,0)$ and $x_2 = (x_1,0)$ where $x_1 = 0.266$ nm. The selected wavelengths are used to calculate a modified infrared slope index employed in smart agriculture for monitoring forests and identifying anomalies in the state of the vegetation cover. The SDL is located in the plane of the z = 0 and has an aperture radius R = 2 mm, maximum height of the microrelief $h_{max} = 4$ µm, number of quantization levels Q = 256.

The relief of the SDL, calculated using formula (1) for the selected parameters, is shown in Fig. 1. When calculating the value of microrelief height h_j are defined in the nodes $u_j = (u_j,v_j)$ of a square grid with a step $\Delta = 2$ µm.

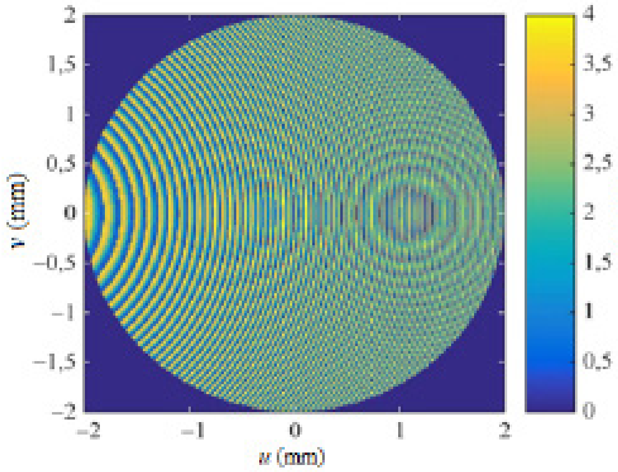

Fig.1. Microrelief of the SDL focusing wavelengths λ_1= 455 nm and λ_2= 750 nm at two points

To assess the efficiency of the SDL, we calculated the intensity distributions formed by the lens using the two-dimensional Fresnel-Kirchhoff integral:

$$I\left(x_j\lambda_1\right)=\left|w\left(x;\lambda_l\right)\right|^2=\left|\frac{1}{\lambda_l f}\iint_G T_{Sl}\left(u;\lambda_l\right)\exp\left\{i\frac{\pi}{\lambda_l f}\left(x-u\right)^2\right\}d^2u\right|^2, \tag{2}$$

where $T_{Sl}(u;\lambda_l)$ is the complex transmittance function of the SDL, $h(u)$, $u \in G$ is the microrelief of the SDL presented in Fig. 1.

It should be noted that the works [18–21] use other integrals for calculation of $I(x_j;\lambda_1)$. Fig. 2,*a* shows the calculated distributions $I_{\text{norm}}(x;\lambda_l)=I(x;\lambda_l)/I_{id}(x_l;\lambda_l)$, normalized to the 'ideal' intensities in focus:

$$I_i\left(x_l;\lambda_l\right)=\left|\frac{\pi R^2}{\lambda_l f}\right|^2, \tag{3}$$

obtained by substituting the complex transmittance functions of the lenses $T_l(u;\lambda_l;x_l)$ in formula (2) instead of the functions $T_{Sl}(u;\lambda_l)$.

Fig. 2,*b* shows sections of two-dimensional distributions along the *x*-axis.

a) *b*)

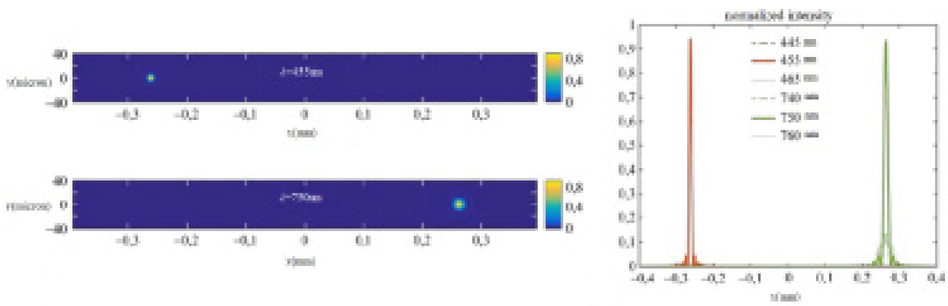

Fig. 2. Normalized two-dimensional intensity distributions formed by the calculated SDL at operating wavelengths λ_1=455 nm (the top) and λ_1=750 nm (the lower) (*a*); sections of normalized intensity distributions along the *x*-axis for wavelengths λ_1, λ_1±10 nm and λ_2, λ_2± 10 nm (*b*)

Water index

Focusing radiation of two relatively close wavelengths λ_1 = 900 nm and λ_2 = 970 nm at two points x_1 = (–x,0), x_2 = (x_1,0), where x_1 = 0.17 mm, located in the plane $z = f$ = 35 mm. The selected wavelengths are used to calculate the water index, which estimates changes in the water content of the vegetation cover [5]. The microrelief of the SDL is calculated using the formula (1), as shown in Fig. 3.

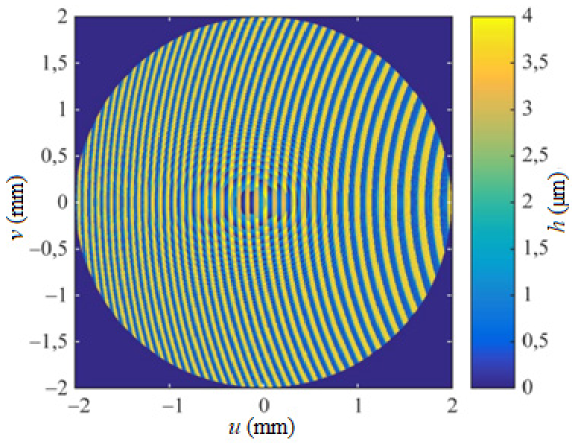

Fig. 3. Microrelief of the SDL, focusing wavelength λ_1 = 900 nm and λ_2 = 970 nm at two points

Fig. 4,*a* shows the normalized distributions $I_{norm}(x;\ \lambda_l)=I(x;\ \lambda_l)/I_{id}(x_l;\ \lambda_l)$, calculated in a rectangular area with cross-sectional dimension $\Delta_y = 3\lambda_2 f/R \approx 50$ μm. These distributions show that the calculated SDL focuses the radiation of the two working wavelengths to specified points. Fig. 4,*b* shows the distributions along the x-axis calculated at wavelengths 890 nm, 910 nm, 960 nm and 980 nm, that differ from the calculated values by ±10 nm. In this example, the operating wavelengths differ by 7.2%. The successful separation of such closely spaced wavelengths using a relatively low diffraction micro-relief with h_{max} = 4 μm is an important result.

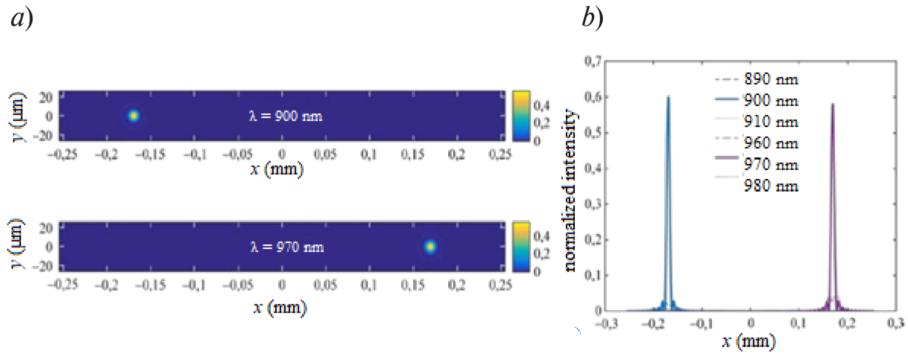

Fig. 4. Normalized two-dimensional intensity distributions formed by the calculated SDL at operating wavelengths λ_1 = 900 nm (the top) and λ_2 = 970 nm (the lower) (*a*); sections of normalized intensity distributions along the x-axis for wavelengths λ_1, λ_1 ± 10 nm and λ_2, λ_2 ± 10 nm (*b*)

Infrared and water indices

In this calculation, four wavelengths were chosen λ_1 = 900 nm, λ_2 = 455 nm, λ_3 = 750 nm and λ_4 = 970 nm to four points x_1 = (–x_1,0), x_2 = (–x_2,0), x_3 = (x_2,0), x_4 = (x_1,0), where x_1 = 0.2 mm, x_2 = 0.1 mm, located in the plane $z = f$ = 35. This SDL can be used to simultaneously obtain information about two vegetation indices, with an aperture radius of R = 2 mm, maximum height of microrelief h_{max} = 6 μm, number of quantization levels Q = 256. The relief of the SDL calculated by the formula (1) is shown in Fig. 5.

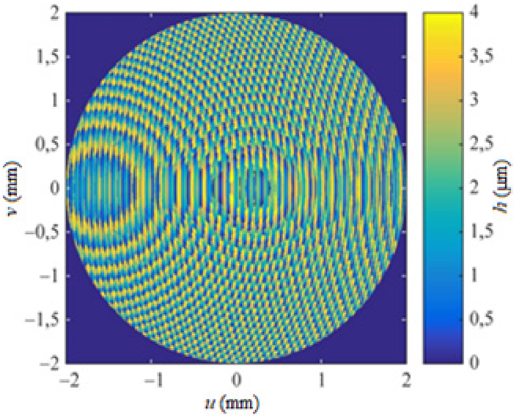

Fig. 5. Microrelief of the SDL focusing wavelengths $\lambda_1 = 900$ nm, $\lambda_2 = 455$ nm, $\lambda_3 = 750$ nm and $\lambda_4 = 970$ nm at four points

Fig. 6,*b* shows cross sections of two-dimensional distributions along the *x*-axis. The maximum values are $0.48I_{id}(x_i;\lambda_l)$, $0.51I_{id}(x_2;\lambda_2)$, $0.56I_{id}(x_3;\lambda_3)$ and $0.47I_{id}(x_4;\lambda_4)$. The width of the focal peaks coincides with the diameter of the diffraction spots with high precision $D_l = 1.22\,\lambda_l f/R$ 'ideal' diffraction lenses. Fig. 6,*b* shows that when the wavelength deviates from one of the calculated values by ±10 nm, there is a significant decrease in the amplitude of the generated intensity distribution (the existing maximum normalized intensities do not exceed 0.025).

a) *b*)

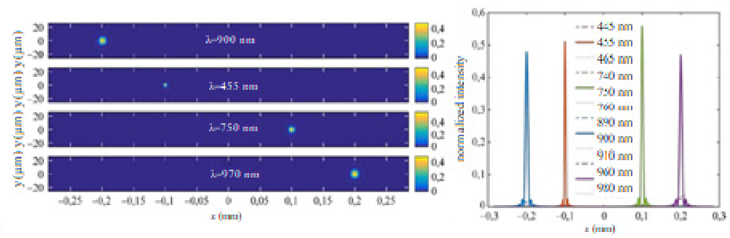

Fig. 6. Normalized two-dimensional intensity distributions formed by the calculated SDL at operating wavelengths $\lambda_1 = 900$ nm (top distribution), $\lambda_2 = 455$ nm (second distribution from the top), $\lambda_3 = 750$ nm (third from the top distribution) and $\lambda_4 = 970$ nm (lower distribution) (*a*); sections of normalized intensity distributions along the *x*-axis for wavelengths λ_1, $\lambda_1 \pm 10$ nm, λ_2, $\lambda_2 \pm 10$ nm, λ_3, $\lambda_3 = 10$ nm and λ_4, $\lambda_4 \pm 10$ nm (*b*)

Conclusion

An analysis of the obtained data shows that the calculated spectral lenses indeed focus the radiation of the operating wavelengths to the specified points, and the widths of the focal peaks coincide with high accuracy with the diameters of diffraction spots of 'ideal' diffractive lenses. This confirms the high efficiency of the developed calculation method. Additionally, the developed technique allows for the reduction of the dimensions of diffractive lenses, which is extremely important when using them in small-sized devices.

REFERENCES

1. **Semenov V.V., Nikiforov N.F., Ermak S.V.,** Calculation of stationary magnetic resonance signal in optically oriented atoms induced by a sequence of radio pulses, Soviet journal of Communications Technology and Electronics. 36(4) (1991) 59–63.

2. **Kuzmin M.S., Rogov S.A.,** On the use of a multi-raster input of one-dimensional signals in two-dimensional optical correlators, Computer Optics. 43(3) (2019) 391–396.

3. **Davydov V.V., Davydova T.I.,** A nondestructive method for express testing of condensed media in ecological monitoring, Russian Journal of Nondestructive Testing. 53(7) (2017) 520–529.

4. **Petrov A.A.,** Digital Frequency Synthesizer for 133Cs-Vapor Atomic Clock, Journal of Communications Technology and Electronics. 62(3) (2017) 289–293.

5. **Myazin N.S., Smirnov K.J.,** Spectral characteristics of InP photocathode with a surface grid electrode, Journal of Physics: Conference Series. 929(1) (2017) 012080.

6. **Logunov S.E., Vysoczky M.G.,** New method of researches of the magnetic fields force lines structure, Journal of Physics: Conference Series. 1038(1) (2018) 012093.

7. **Kuzmin M.S., Rogov S.A.,** Experimental study of a joint-transform correlator, Quantum Electronics. 48(11) (2018) 1048–1054.

8. **Smirnov K.J., Glagolev S.F., Tushavin G.V.,** High speed near-infrared range sensor based on InP/InGaAs heterostructures, Journal of Physics: Conference Series. 1124(2) (2018) 022014.

9. **Grebenikova N.M., Smirnov K.J., Rud V.Yu., Artemiev V.V.,** Features of monitoring the state of the liquid medium by refractometer, Journal of Physics: Conference Series. 1135(1) (2018) 012055.

10. **Davydov V.V., Kruzhalov S.V.,** Method for Determining Defects on the Inner Walls of Tubing from the Velocity Distribution of the Flowing Fluid, Measurement Techniques. 61(4) (2018) 365–372.

11. **Mazing M.S., Zaitceva A.Y., Kislyakov Y.Y., Kondakov N.S., Avdyushenko S.A.,** Analytical complex for study of the oxygen status of tissues of the human organism, Journal of Physics: Conference Series. 1695(1) (2020) 012065.

12. **Davydov V., Gureeva I., Davydov R., Dudkin V.,** Flowing Refractometer for Feed Water State Control in the Second Loop of Nuclear Reactor. Energies. 15(2) (2022) 457.

13. **Sweeney D.W., Sommargren G.E.,** Harmonic diffractive lenses. Applied Optics. 34(14) (1995) 2469–2475.

14. **Davydov V.V., Kruzhalov S.V., Vologdin V.A.,** Concerning some features of studying the flow of liquid media by a Doppler method, Journal of Optical Technology (A Translation of Opticheskii Zhurnal). 84(8) (2017) 568–573.

15. **Rossi M., Kunz R. E., Herzig H.P.,** Refractive and diffractive properties of planar micro-optical elements. Vol. 34, Applied Optics. 34(26) (1995) 5996–6007.

16. **Faklis D., Morris G.M.,** Spectral properties of multiorder diffractive lenses. Applied Optics. 34(14) (1995) 2462–2468.

17. **Bannari A., Morin D., Bonn F., Huete A.R.,** A review of vegetation indices. Vol. 13, Remote Sensing Reviews. 13 (1995) 95–120.

18. **Byzov E.V., Doskolovich L.L, Kravchenko S.V., Moiseev M.A., Kazanskiy N.L.,** Design of optical elements for an extended light source. Computer Optics, 2023, 47(1) 40–47.

19. **Doskolovich L.L., Mingazov A.A., Byzov E.V., Bykov D.A., Bezus E.A.,** Method for calculating the eikonal function and its application to design of diffractive optical elements for optical beam shaping. Computer Optics, 2022, 46(2) 173–183.

20. **Blank V., Skidanov R, Doskolovich L., Kazanskiy N.,** Spectral diffractive lenses for measuring a modified red edge simple ratio index and a water band index. Sensors, 2021, 21(22), 7694.

21. **Bezus E.A., Bykov D.A., Doskolovich L.L.,** Integrated Gires–Tournois interferometers based on evanescently coupled ridge resonators. Optics Letters, 2020, 45(18) 5065–5068.

THE AUTHOR

GORANSKAIA Svetlana A.
svetlancho.zueva@yandex.ru
ORCID: 0009-0004-3728-9837

Received 01.07.2023. Approved after reviewing 24.07.2023. Accepted 26.07.2023.